Journal of the Iranian Chemical Society (2018) 15:1625–1632
https://doi.org/10.1007/s13738-018-1360-9

ORIGINAL PAPER

Immobilized different amines on modified magnetic nanoparticles as catalyst for biodiesel production from soybean oil

Faezeh Farzaneh[1] · Zahra Mohammadi[1] · Zahra Azarkamanzad[1]

Received: 20 February 2018 / Accepted: 4 April 2018 / Published online: 14 May 2018

Abstract
Fe_3O_4 nanoparticles were modified with tetraethylorthosilicate (TEOS) and (3-chloropropyl)trimethoxysilane (CPTMS) followed by immobilization with different amines such as guanine, piperazine, methylamine, morpholine, aniline, ethylenediamine, 3-aminopropyltriethoxysilane, and melamine, designated as Fe_3O_4@SiO_2@CPTMS@amine (nanocatalyst). The prepared nanocatalysts were characterized by means of FTIR, XRD, VSM, SEM, and TEM. *Trans*-esterification reactions of soybean oil with methanol were then carried out in the presence of the Fe_3O_4@SiO_2@CPTMS@amine as a nanocatalyst. Optimization of the reaction parameters revealed that the fatty acid methyl esters (FAMEs or biodiesel) is obtained in 6–96% yields by using methanol to oil molar ratio of 36 in the presence of 6% of nanocatalysts containing melamine and guanine, respectively, at 160 °C within 3 h. The stability and reusability of the catalyst as well as the effect of reaction parameters on the FAME yield are described in this paper.

Keywords Modified magnetic nanoparticles · Amines · Biodiesel production

Introduction

Magnetic nanoparticles with uniform size distribution are of interest because of their extensive applications in magnetically controlled drug delivery, memory storage devices, MRI, sensors, and catalysis [1–4]. In fact, the immobilization of the catalytically active species on the surface of modified magnetic nanoparticles is a suitable method because of the easy catalyst separation by applying an external magnetic field [5–8]. Recovery and reuse of catalysts after catalytic reactions are also important factors for sustainable process management. Directed functionalization of the surfaces of nanosized magnetic materials is an elegant way to bridge the gap between heterogeneous and homogeneous catalysis systems. Several organic reactions such as olefin epoxidation, decarboxylative coupling, and hydrogenation reactions have been carried out using catalysts immobilized on nanomagnetic particles as support [9–14]. In this study, attempt has been made on the modification of nanomagnetic particles with different amines for biodiesel production.

Biodiesel is a mixture of fatty acid methyl esters (FAMEs), produced by *trans*-esterification of triglycerides with methanol or other short-chain alcohols in the presence of an appropriate catalyst [15–18]. Due to the cost of fossil fuels to energy crisis as well as environmental pollutions, global warming, and greenhouse gas emission, an alternative and renewable source of energy has become more attractive in recent years. Not only biodiesel is a biodegradable fuel, non-toxic, and free of sulfur and carcinogenic compounds, it is also is a cleaner burning fuel than petrol and diesel. *Trans*-esterification reactions for production of biodiesel are commonly catalyzed by acids or bases in homogeneous or heterogeneous systems [19]. It was found that the biodiesel production in basic media is more common than acidic [20–23]. Heterogeneous catalysts with high catalytic performance in the synthesis of biodiesel are also environmentally friendly and are removable and reusable [24]. Nowadays, a wide variety of heterogeneous catalysts including microporous [25–27], or mesoporous materials [28], heteropolyacids [29], coordination polymers [30], metal organic frameworks [31–33], and finally oxides or mixed oxides nanocomposites

Electronic supplementary material The online version of this article (https://doi.org/10.1007/s13738-018-1360-9) contains supplementary material, which is available to authorized users.

✉ Faezeh Farzaneh
faezeh_farzaneh@yahoo.com; farzaneh@alzahra.ac.ir

[1] Department of Chemistry, Faculty of Physics and Chemistry, Alzahra University, P.O.Box 1993891176, Vanak, Tehran, Iran

have been investigated as catalyst for production of biodiesel using *trans*-esterification reactions [34–36].

Experimental

Materials and physical measurements

All materials were of commercial reagent grade and used without further purification. Methanol, tetraethyl orthosilicate, sodium chloride, ferric chloride, ferrous chloride tetrahydrate, ammonia (25% in water), glycerol, acetic acid, ethanol, potassium chloride, (3-chloropropyl)trimethoxysilane, guanine, melamine, morpholine, ethylenediamine, methyl amine, aniline, piperazine, diethyl ether, sodium hydride, and 3-aminopropyltrimethoxysilane were obtained from Merck Chemical Company. Commercial edible soybean oil was obtained from local grocery store with the average molecular weight of 881 g/mol (calculated from the saponification value S.V. = 190 mg KOH/g, with acid value and water contents of 0.4 mg KOH/g and 96.7 mg/kg, respectively).

The X-ray diffractions (XRD) were recorded on a Siefert 3003 PTS diffractometer using Cu Kα radiation ($k = 0.15406$ nm). FTIR spectra were recorded by Bruker Tensor 27 FTIR spectrometer device in the range of 4000–400 cm^{-1} with KBr pellet (5 mg sample with 100 mg KBr). Vibrating sample magnetometer (VSM) using the (BHV-55, Riken, Japan) with magnetic fields in the range − 8000 to 8000 Oe was conducted at room temperature. To see the reaction efficiency, GC Agilent 6890 series equipped with a flame ionization Detector FID detector, HP-5, 5% phenylmethylsiloxane capillary was used. Biodiesel composite was determined by Agilent 5973 network, mass selective detector, HP-5 MS 6989 network GC system. The morphology and particle size of the prepared nanocomposites were determined by scanning electron microscopy (SEM) images with model KYKY-EM3200-26 kV. Transmission electron microscopy (TEM) images were taken by Zeiss-EM10C-100 kV.

Preparation of Fe_3O_4@SiO_2@CPTMS

Silica-coated Fe_3O_4 magnetic nanoparticles (SCMNPs) were prepared according to the previously reported procedure [37] (see also supplementary materials). The silica-coated magnetic nanoparticles SCMNPs (2 g) were suspended in ethanol (100 mL), and then (3-chloropropyl)trimethoxysilane (CPTMS) (2 mL) was added under nitrogen atmosphere. The mixture was heated at reflux for 12 h. The resultant solid was magnetically separated, washed with methanol in order to remove the unreacted residue of silylation reagent [37, 38].

Preparation of Fe_3O_4@SiO_2@CPTMS@ amines

To a suspension of Fe_3O_4@SiO_2@CPTMS (2 g) in ethanol (100 mL) were added amine (2 mmol) and KOH (0.1 g) dissolved in H_2O (10 mL). The mixture was heated at reflux under nitrogen atmosphere for 12 h. The resultant solid was then magnetically separated, washed with methanol in order to remove the unreacted residue of silylation reagent.

Trans-esterification of soybean oil, general procedure

Trans-esterification reactions with different amines immobilized on modified magnetic nanoparticles were carried out in an autoclave with a mechanical stirrer. The catalyst (0.06 g) was dispersed in MeOH (3.2 mL), followed by the addition of soybean oil (5 mL) with the average molecular weight of 881 g/mol to the reaction mixture. After stirring for 2 h at 160 °C, the reaction mixture was cooled to room temperature. The catalyst was then separated using a magnet and washed with *n*-hexane. After evaporation of the solvent under reduced pressure, the two layers containing methyl esters, soybean oil, mono- and diglycerides in the upper, and glycerol in the lower phases were separated by a decanter. The FAME content was then determined by GC and GC/Mass analysis [39].

Results and discussion

Fe_3O_4@SiO_2@CPTMS@amines were prepared according to the procedure presented in Scheme 1.

Magnetic nanoparticles (MNPs) were initially prepared by precipitation of iron (II) and iron (III) ions in a basic solution. Subsequently, silica was coated on Fe_3O_4 to form Fe_3O_4@SiO_2 core–shell particles using TEOS in acidic solution to prevent the aggregation and increase in the stability of Fe_3O_4 nanoparticles [37]. The modification of magnetic nanoparticles surface is generally carried out by functionalization with desired organic groups [38, 39]. Therefore, after the surface functionalization with CPTMS, different amines such as guanine, piperazine, methylamine, morpholine, aniline, ethylenediamine, 3-aminopropyltriethoxysilane, and melamine were immobilized and designated as Fe_3O_4@SiO_2@CPTMS@amines (Scheme 1).

The FTIR spectra of Fe_3O_4@SiO_2@CPTMS, guanine, and Fe_3O_4@SiO_2@CPTMS@guanines are presented in Fig. 1a–c, respectively. As indicated in Fig. 1a, the bands appearing at 448 and 579 cm^{-1} are attributed to the Fe–O vibrations and the band displaying at 1090 cm^{-1} is due to Si–O vibration. Two obvious bands appearing at 2870 and

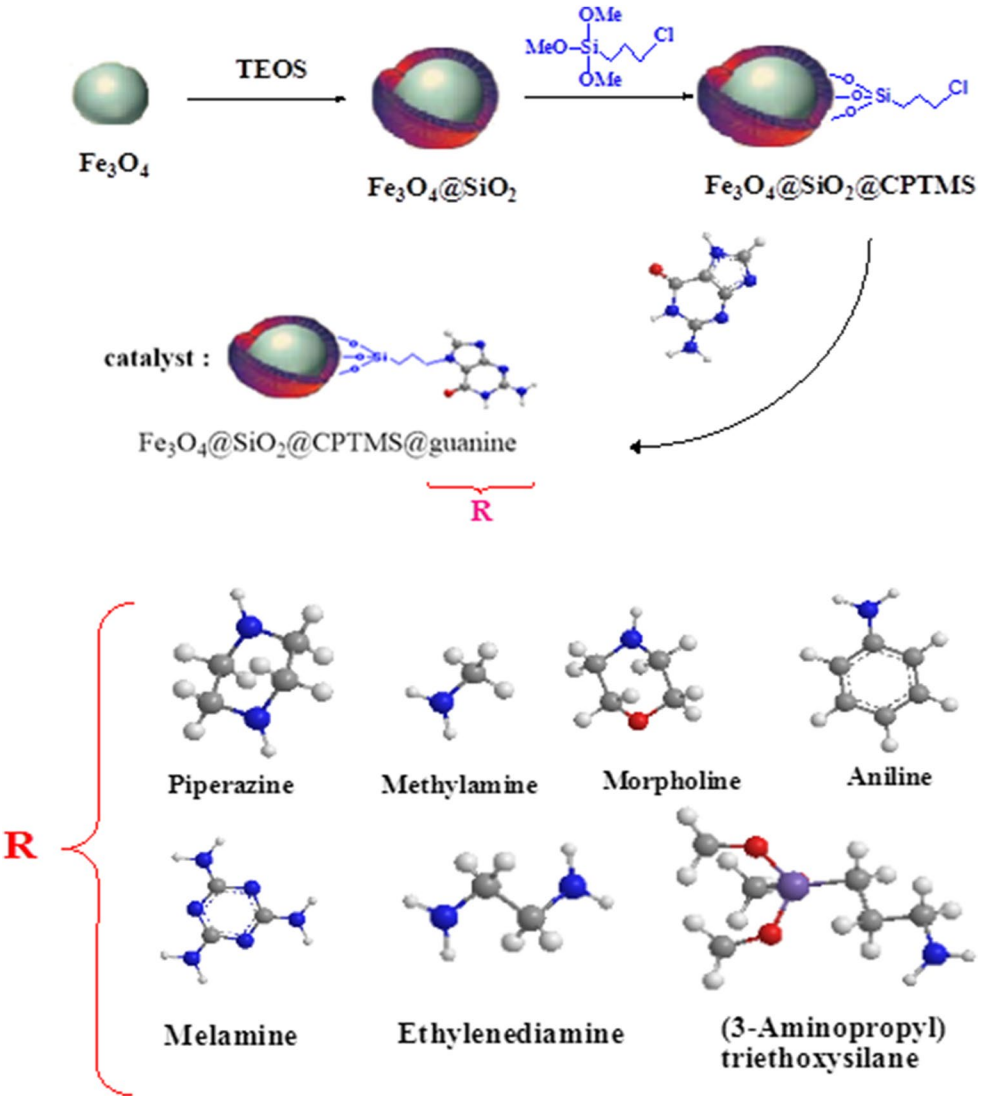

Scheme 1 Preparation steps of Fe_3O_4@SiO_2@CPTMS@amines

2920 cm^{-1} are associated with C–H stretching vibrations of CPTMS immobilized on nanomagnet consistent with the predicted structure of Fe_3O_4@SiO_2@CPTMS (Fig. 1c) [40]. Appearance of two bands around 3422–3100 cm^{-1} is due to the NH stretching vibrations of guanidine (Fig. 1b). A strong peak displaying at 1700 cm^{-1} due to the C=O vibrations is observed for guanine spectra before and after immobilization (Fig. 1b, c) [40–44]. The FTIR spectra for other amines such as piperazine, methylamine, morpholine, aniline, ethylenediamine, 3-aminopropyltriethoxysilane, and melamine are included in supplementary (Fig. S1). Comparison of the amines vibrations before and after immobilization confirmed the presence of immobilized amines (see supplementary Fig. S1a–h).

The XRD patterns of the prepared Fe_3O_4, Fe_3O_4@SiO_2, Fe_3O_4@SiO_2@CPTMS, Fe_3O_4@SiO_2@CPTMS@guanine before and after the reaction are shown in Fig. 2. The diffraction peaks with 2θ values at 22°, 35°, 42°, 54°, 57° observed for Fe_3O_4 nanoparticles are related to the 220, 311, 411, 422, and 522, respectively. These results are consistent with those of the standard JCPDS card No. 190629 for iron oxide. The similarity observed in the XRD patterns of Fe_3O_4@SiO_2@CPTMS and Fe_3O_4@SiO_2@CPTMS@guanine indicates no change after immobilization of the amines (Fig. 2c, d).

The nanomagnetic properties of the prepared catalyst containing a magnetite component were studied by a VSM at 300 °K. The magnetization curves of Fe_3O_4, Fe_3O_4@SiO_2@CPTMS, Fe_3O_4@SiO_2@CPTMS@guanine before and after using as catalyst are shown in Fig. 3a–d, respectively. It was found that the magnetization saturated with iron oxide which was determined as 61 emu/g reduced to 57 emu/g when it was coated with silica. This reduction is due to coated with the silica. Before and after reaction, the magnetization is reduced to 42 and then 32 emu/g, which indicates that the catalyst has still superparamagnetic character.

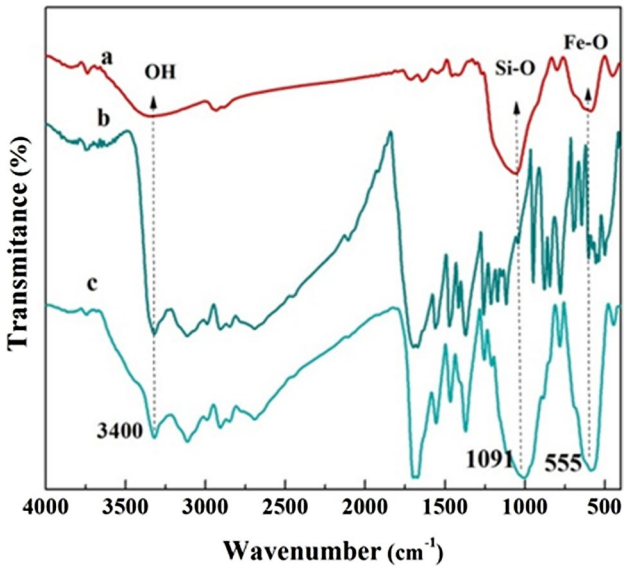

Fig. 1 FTIR spectra of Fe_3O_4@SiO_2@CPTMS, guanine, and Fe_3O_4@SiO_2@CPTMS @guanine

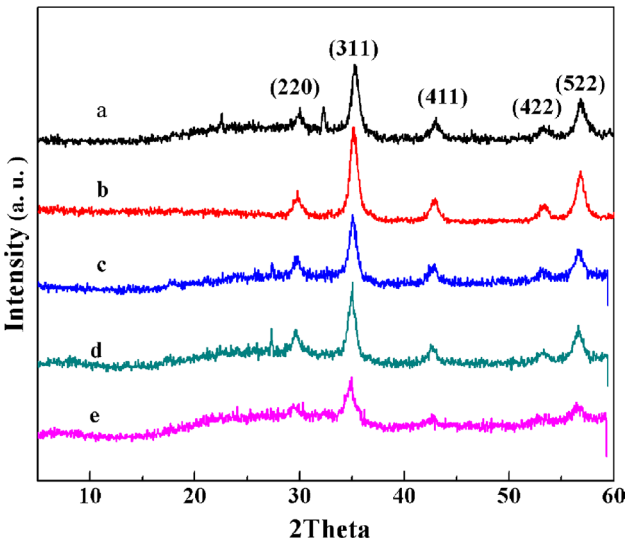

Fig. 2 XRD patterns for **a** Fe_3O_4, **b** Fe_3O_4@SiO_2, **c** Fe_3O_4@SiO_2@CPTMS, **d** Fe_3O_4@SiO_2@CPTMS@guanine before, **e** after using as catalyst

The SEM and TEM images of Fe_3O_4@SiO_2@CPTMS@guanine are shown in Fig. 4a, b, respectively. The SEM image shows the formation particles sizes between 45 and 65 nm (Fig. 4a). The formation of core and shell particles is evident in TEM image (Fig. 4b).

Investigation of the FTIR spectra of piperazine, methylamine, morpholine, aniline, ethylenediamine, 3-aminopropyltriethoxysilane, and melamine designated as Fe_3O_4@SiO_2@CPTMS@amines (Scheme 1) (shown in

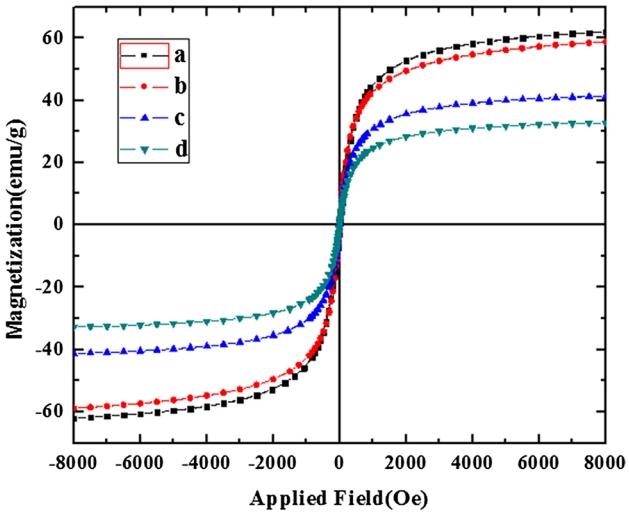

Fig. 3 Magnetization curves of **a** Fe_3O_4, **b** Fe_3O_4@SiO_2@CPTMS, **c** Fe_3O_4@SiO_2@CPTMS@guanine before, **d** after using as catalyst

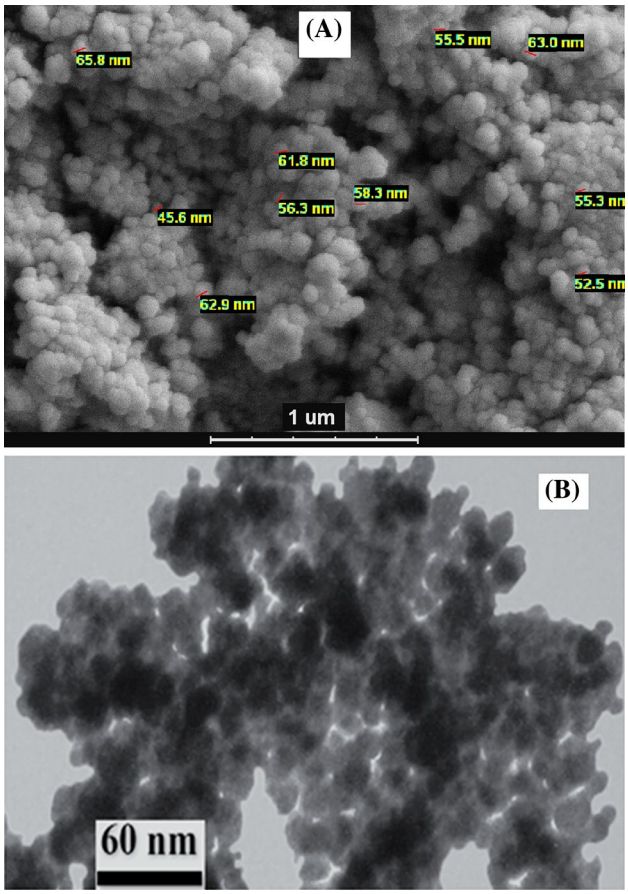

Fig. 4 **a** SEM, **b** TEM images of Fe_3O_4@SiO_2@CPTMS@guanine

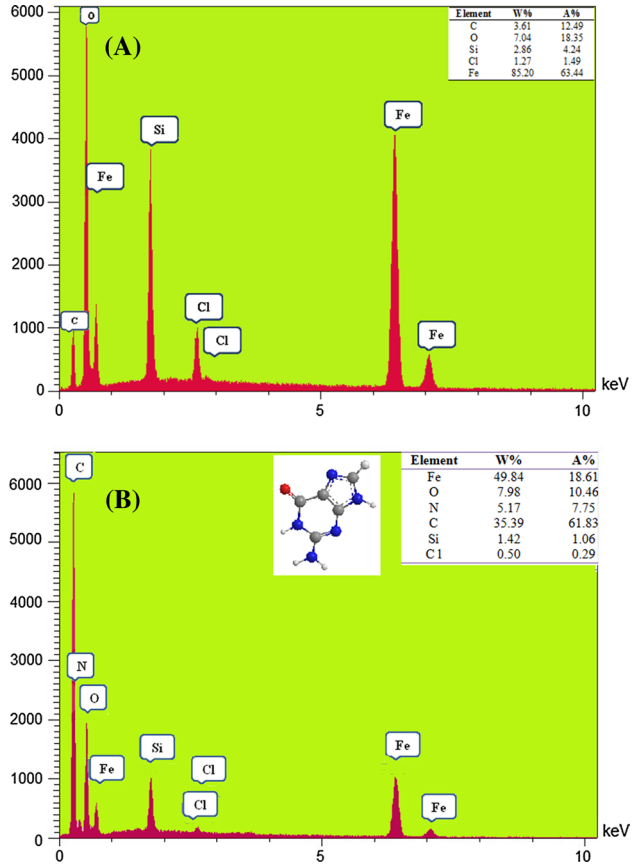

Fig. 5 EDX patterns of Fe_3O_4@SiO_2@CPTMS and Fe_3O_4@SiO_2@CPTMS@guanine

supplementary, Fig. S1) indicates that the immobilization of these amines has been carried out succesfully. Moreover, modification of the iron oxide nanoparticles is confirmed on the basis of a decrease in the chlorine amount and the presence of nitrogen after immobilization of the desired organic amines based on the EDX results presented in Fig. 5 and Figs. S2–S7. Recall that the amount of nitrogen and chlorine depends on the amine type as indicated in supplementary (Figs. S2–S7).

Optimization of *trans*-esterification reaction parameters

In order to optimize the biodiesel yield, the effect of the amount of catalyst (based on the soybean oil weight), reaction time, methanol to oil molar ratio, and reaction temperature was investigated. As indicated in Fig. 6, there is a direct relation between the oil conversion and the amount of catalyst when the reaction is heated at reflux for 6 h. Significantly, *trans*-esterification reaction proceeded with 96% oil conversion together with the maximum formation of biodiesel in the presence of 6% catalyst.

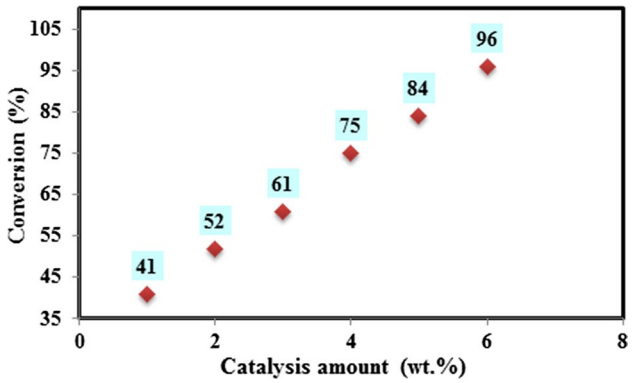

Fig. 6 Influence of catalysis amount on biodiesel yield at 160 °C within 3 h

Reaction temperature is also effective on the reaction rate as well as the biodiesel yield because the rate constant intrinsically depends on temperature. Notably, an increase in oil conversion from 16 to 96% was observed within 3 h when reaction temperature was marginally increased from 80 to 160 °C (Fig. 7).

It was also found that increasing the reaction time from 30 min to 3 h increased the reaction conversion from 34 to 96% (Fig. 8).

The effect of methanol to oil molar ratio shown in Fig. 9 reveals that increasing the molar ratio from 6:1 to 36:1 enhances the oil conversion from 6 to 96%. Therefore, the stoichiometry of *trans*-esterification reaction requires 3 mol of methanol per 1 mol of biodiesel and glycerol. Utilization of an excess amount of methanol seems to shift the equilibrium toward the product. Moreover, the excess of methanol accelerates the removal of the biodiesel product from the catalyst surface in order to regenerate the active sites.

The catalytic effect of immobilized amines of guanidine, piperazine, methylamine, morpholine, aniline,

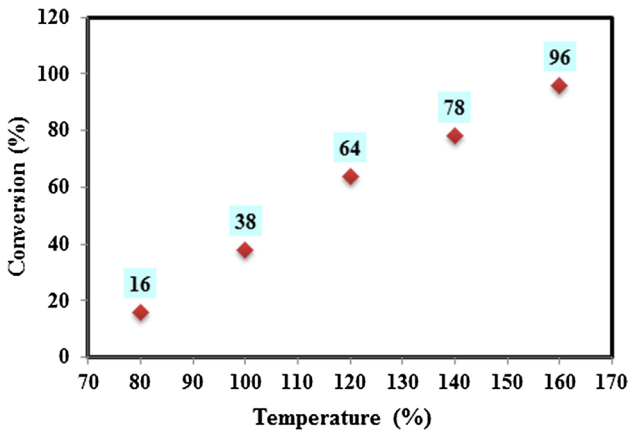

Fig. 7 Effect of reaction temperature on biodiesel yield. Reaction conditions: catalyst amount 6 wt %; methanol/oil ratio, 36:1. Time 3 h

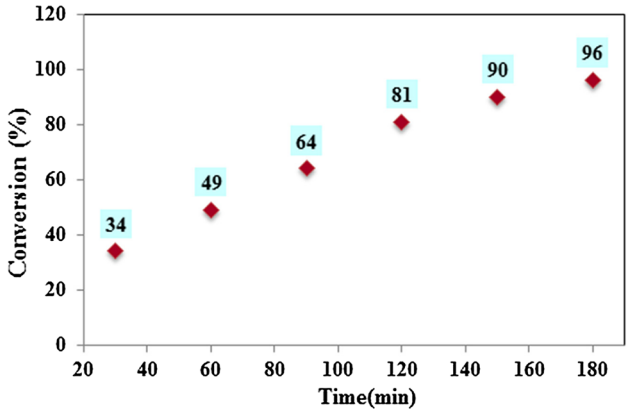

Fig. 8 Influence of time on biodiesel yield with 6% catalyst, at 160 °C with methanol/oil molar ratio 36:1

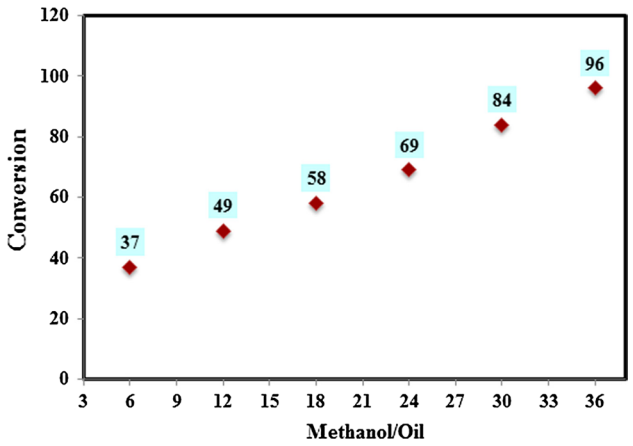

Fig. 9 Influence of methanol/oil molar ratio on biodiesel yield with 6% catalyst amount (based on the soybean oil weight) at 160 °C

ethylenediamine, 3-aminopropyltriethoxysilane, and melamine on modified magnetic nanoparticles on the biodiesel production is given in Table 1. As seen in this table, the yield of reaction depends on the amine basicity (Table 1) since catalysts containing the most and least basic amines of guanine and melamine afforded the highest and lowest yields of biodiesel, respectively.

On the other hand, based on EDX results, no potassium ions were detected on the nanocomposite. The other point is the chlorine percent decreased after each immobilization. In which for immobilization of guanine, about 40% of Cl has been exchanged. The total distribution of methyl esters is given in Table 1. In fact, the product distribution of methyl esters in biodiesel production for different amines is the same, but the conversions are different.

In order to investigate the heterogeneity character of the prepared catalyst, the solid catalyst was recovered by external magnet from reaction mixture after completion of the first run and reusability of the catalyst was investigated in another run by addition of fresh soybean oil and methanol similar to the initial reaction. A little decrease in catalyst activity from 98% to the 96% was found. On the other hand, the filtrate of the reaction mixture after first run did not show any activity, which means no desorption was observed due to the course of reaction. The FTIR, XRD, and VSM patterns of prepared catalyst before and after using as catalyst were similar as shown in Figs. 1c, 2e, and 3d, respectively.

Reaction mechanism

The proposed mechanism for the Fe_3O_4@SiO_2@CPTMS@amine-catalyzed *trans*-esterification reaction of soybean oil with methanol is presented in Scheme 2. Addition of the initially generated CH_3O^- via an acid–base reaction of CH_3OH with catalyst at the triglyceride carbonyl group affords a tetracoordinate carbon atom. Protonation of the tetracoordinated intermediate by proton donor catalyst-H^+ followed by proton transfer and alcohol elimination step results in the formation of FAME [45].

Table 1 Effect of different organic amines immobilized on Fe_3O_4@SiO_2@CPTMS (nanocatalyst)

Immobilized amines	Conversion (%)	Product distribution (%)		
		Methyl palmitate	Methyl linoleate	Methyl oleate
Guanine	96	12.65	84.31	4.93
Piperazine	76	12.93	83.82	3.24
APTMS	64	11.30	83.63	4.36
EDA	80	11.91	83.04	4.75
Methylamine	84	11.60	83.63	4.80
Morpholine	16	12.33	85.68	–
Aniline	18	12.23	85.54	–
Melamine	6	12.11	86.00	–

Reactions conditions: catalyst amount (6 wt%); methanol/oil ratio (36:1); temperature (160 °C); and time (3 h)

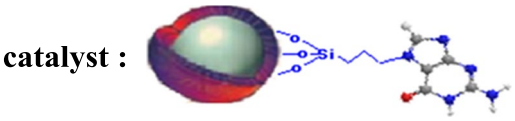

$Fe_3O_4@SiO_2@CPTMS@guanine$

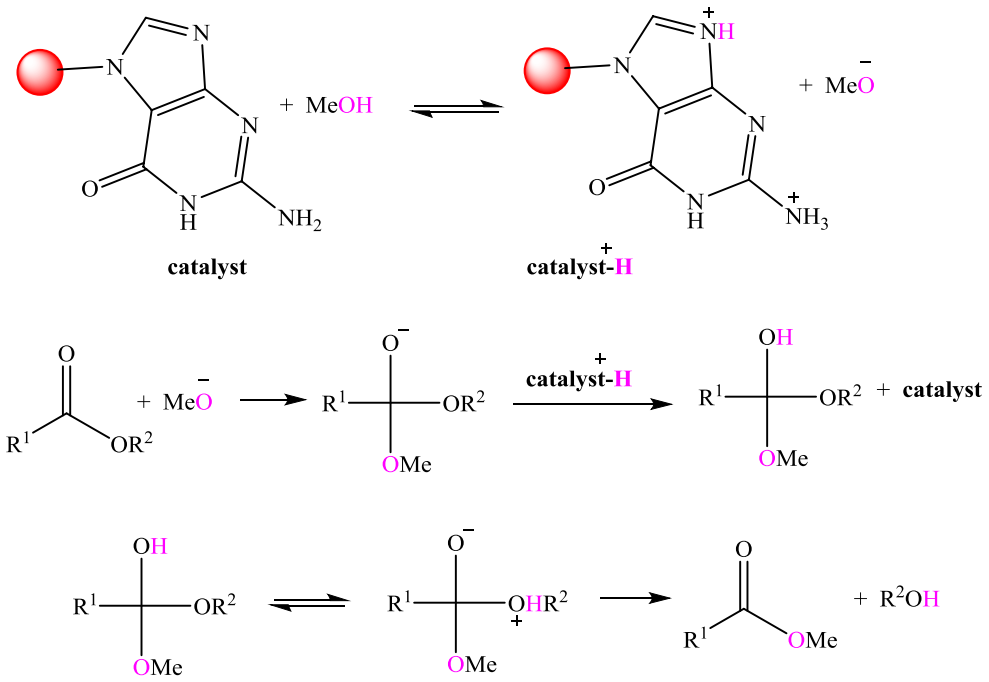

Scheme 2 Proposed mechanism for biodiesel production

Conclusion

In this study, magnetic nanoparticles were modified with TEOS and CPTMS followed by immobilization with guanine, piperazine, methylamine, morpholine, aniline, ethylenediamine, 3-aminopropyltriethoxysilane, and melamine. The modified nanomagnets were then used as catalyst for biodiesel production. It was found that guanidine and melamine show the most and least activity to biodiesel production under optimum conditions.

Acknowledgements The financial support from the Alzahra University is gratefully acknowledged.

References

1. R. Hao, R. Xing, Z. Xu, Y. Hou, S. Gao, S. Sun, Adv. Mater. **22**, 2729 (2010)
2. I. Brigger, C. Dubernet, P. Couvreur, Adv. Drug. Deliv. Rev. **54**, 631 (2002)
3. A.K. Gupta, M. Gupt, Biomaterials **26**, 3995 (2005)
4. B. Shen, Y. Wang, Z. Wang, React. Kinet. Mech. Catal. **101**, 387 (2010)
5. A.H. Lu, E.L. Salabas, F. Schüth, Angew. Chem. Int. Ed. **46**, 1222 (2007)
6. R.N. Grass, E.K. Athanassiou, W.J. Stark, Angew. Chem. Int. Ed. **46**, 4909 (2007)
7. A.H. Lu, W. Schmidt, N. Matoussevitch, H. Bonnemann, B. Spliethoff, B. Tesche, E. Bill, W. Kiefer, F. Schuth, Angew. Chem. Int. Ed. **43**, 4303 (2004)
8. S.C. Tsang, V. Caps, I. Paraskevas, D. Chadwick, D. Thompsett, Angew. Chem. Int. Ed. **43**, 5645 (2004)
9. K.M. Yeo, S.I. Lee, Y.T. Lee, Y.K. Chung, I.S. Lee, Chem. Lett. **37**, 116 (2008)
10. M. Shokouhimehr, Y. Piao, J. Kim, Y. Jang, T. Hyeon, Angew. Chem. Int. Ed. **46**, 7039 (2007)
11. W.-R. Huck, T. Bürgi, T. Mallat, A. Baiker, J. Catal. **216**, 276 (2003)
12. R. Abu-Reziq, D. Wang, M. Post, H. Alper, Adv. Synth. Catal. **349**, 2145 (2007)
13. M.J. Jacinto, P.K. Kiyohara, S.H. Masunaga, R.F. Jardim, L.M. Rossi, Appl. Catal. A Gen. **338**, 52 (2008)
14. S. Shylesh, V. Schünemann, W.R. Thiel, Angew. Chem. Int. Ed. **49**, 3428 (2010)
15. Y. Yan, X. Li, G. Wang, X. Gui, G. Li, F. Su, Appl. Energy **113**, 1614 (2014)

16. P.D. Patil, V.G. Gude, Sh Deng, Ind. Eng. Chem. Res. **34**, 10850 (2009)
17. C.R. Coronado, J.A. Carvalho, J.L. Silveira, Fuel Process. Technol. **90**, 204 (2009)
18. H. Lu, X. Yu, Sh Yang, H. Yang, Sh Tung Tu, Fuel **165**, 215 (2016)
19. A. SivasamyKien, Y. Cheah, P. Fornasiero, F. Kemausuor, S. Zinoviev, S. Miertus, ChemSusChem **2**, 278 (2009)
20. J.M. Marchetti, V.U. Miguel, A.F. Errazu, Renew. Sustain. Energy Rev. **11**, 1300 (2007)
21. D.Y.C. Leung, X. Wu, M.K.H. Leung, Appl. Energy **87**, 1083 (2010)
22. M.R. Shahbazi, B. Khoshandam, M. Ghazvini Nasiri, J. Taiwan Ins. Chem. Eng. **43**, 504 (2012)
23. A. Demirbas, Energy Convers. Manag. **49**, 125 (2008)
24. A.F. Lee, J.A. Bennett, J.C. Manayil, L. Wilson, Chem. Soc. Rev. **43**, 7887 (2014)
25. S.S. Vieira, Z.M. Magriotis, N.A.V. Santos, A.A. Saczk, C.E. Hori, P.A. Arroyo, Bioresour. Technol. **133**, 248 (2013)
26. A. Carrero, G. Vicente, R. Rodriguez, M. Linares, G.L. del Peso, Catal. Today **167**, 148 (2011)
27. M.J. Ramos, A. Casas, L. Rodrıguez, R. Romero, A. Perez, Appl. Catal. A Gen. **346**, 79 (2008)
28. M.C. Albuquerque, I. Jiménez-Urbistondo, J. Santamaría-González, J.M. Mérida-Robles, R. Moreno-Tost, E. Rodríguez-Castellón, A. Jiménez-López, D.C. Azevedo, C.L. Cavalcante Jr., P. Maireles-Torres, Appl. Catal. A Gen. **334**, 35 (2008)
29. K. Narasimharao, D.R. Brown, A.F. Lee, A.D. Newman, P.F. Siril, S.J. Tavener, K. Wilson, J. Catal. **248**, 226 (2007)
30. F. Farzaneh, F. Moghzil, E. Rashtizadeh, React. Kinet. Mech. Catal. **118**, 509 (2016)
31. A. Nikseresht, A. Daniyali, M. Ali-Mohammadi, A. Afzalinia, A. Mirzaie, Ultrason. Sonochem. **37**, 203 (2017)
32. H. Wan, C. Chen, Z. Wu, Y. Que, Y. Feng, W. Wang, L. Wang, G. Guan, X. Liu, ChemCatChem **7**, 441 (2015)
33. L.H. Wee, N. Janssens, S.R. Bajpe, C.E.A. Kirschhock, J.A. Martens, Catal. Today **171**, 275 (2011)
34. E. Rashtizadeh, F. Farzaneh, J. Taiwan Inst. Chem. Eng. **44**, 917 (2013)
35. E. Rashtizadeh, F. Farzaneh, Z. Talebpour, Bioresour. Technol. **154**, 32 (2014)
36. F. Farzaneh, B. Dashtipour, E. Rashtizadeh, J. Sol–Gel Sci. Technol. **81**, 859 (2017)
37. X. Liu, Z. Ma, J. Xing, H. Liu, J. Magn. Magn. Mater. **270**, 1 (2004)
38. Z. Asgharpour, F. Farzaneh, A. Abbasi, RSC Adv. **6**, 95729 (2016)
39. M.Z. Kyari, Int. Agrophys. **22**, 139 (2008)
40. Z. Wang, B. Shen, Z. Aihua, N. He, Chem. Eng. J. **113**, 27 (2005)
41. H. Cao, J. He, L. Deng, X. Gao, Appl. Surf. Sci. **255**, 7974 (2009)
42. J. Wang, S. Zheng, Y. Shao, J. Liu, Z. Xu, D. Zhu, J. Colloid Interface Sci. **34**, 9293 (2010)
43. M. Masteri-Farahani, N. Tayyebi, J. Mol. Catal. A **348**, 83 (2011)
44. L. Hamidipour, F. Farzaneh, M. Ghandi, React. Kinet. Mech. Catal. **107**, 421 (2012)
45. X. Liu, H. He, Y. Wang, Catal. Commun. **8**, 1107 (2007)